Procoagulant platelet sentinels prevent inflammatory bleeding through GPIIBIIIA and GPVI – Supplementary Information.

Rainer Kaiser[1,2*], Raphael Escaig[1,2], Jan Kranich[3], Marie-Louise Hoffknecht[1], Afra Anjum[1,2], Vivien Polewka[1], Magdalena Mader[1,2], Wenbo Hu[3], Larissa Belz[1], Christoph Gold[1,2], Anna Titova[1], Michael Lorenz[1], Stefan Kääb[1,2], Kami Pekayvaz[1,2], Florian Gaertner[1,2], Konstantin Stark[1,2], Thomas Brocker[3], Steffen Massberg[1,2] and Leo Nicolai[1,2*]

[1]Medizinische Klinik und Poliklinik I University Hospital Ludwig-Maximilian University, Munich, Germany
[2]DZHK (German Centre for Cardiovascular Research), partner site Munich Heart Alliance, Germany
[3]Institute for Immunology, Biomedical Center, Medical Faculty, Ludwig-Maximilian University Munich, 82152 Planegg-Martinsried, Germany

*Correspondence to rainer.kaiser@med.uni-muenchen.de and leo.nicolai@med.uni-muenchen.de, Medizinische Klinik und Poliklinik I, University Hospital Ludwig-Maximilian-University Munich, Marchioninistr. 15 81377, Munich, Germany.

Table of contents

- Suppl. Methods
- Suppl. Tables 1+2
- Suppl. Figures and Suppl. Figure captions S1-9
- Suppl. Videos and Suppl. Video captions 1-3
- Suppl. References

Supplementary Methods

Mouse strains

C57BL/6J (Stock No: 000664, labeled Bl6 or wild-type/WT), PF4cre[1] and CypD$^{fl/fl}$ (Ppif^{tm1Mmos}/J, Stock No: 005737) mice were purchased from The Jackson Laboratory and maintained at our animal facility. The TMEM16F$^{fl/fl}$ line was provided by the RIKEN BioResource Center (BRC) through the National BioResource Project of the Ministry of Education, Culture, Sports, Science and Technology (MEXT)/Agency for Medical Research and Development (Japan)[2,3]. Arpc2$^{fl/fl}$ were gifts from Rong Li and the Wellcome Trust Sanger Institute, respectively. All strains used in this study were backcrossed to C57BL/6J background. Mice of both sexes were used for *in vitro* studies and tail bleeding assays. For acute lung injury, intraperitoneal sepsis and mesentery live imaging models, female mice were used, while male mice were used for the arterial thrombosis model. Unless otherwise stated, mice were 8 to 14 weeks of age when entering experiments.

Mouse anesthesia

Anesthesia was performed by intraperitoneal injection of medetomidine (0.5 mg/kg body weight), midazolam (5 mg/kg body weight) and fentanyl (0.05 mg/kg body weight, MMF) after initial induction with isoflurane. Anesthetized mice were kept on heating pads, where depth of anesthesia was monitored by toe pinching reflexes and breathing patterns. To maintain narcosis, repeated s.c. injections of 25-50% of the induction dose was applied.

Intraperitoneal sepsis model and evaluation of peritoneal bleeding

Mice were injected with 1 mg/kg BW LPS intraperitoneally and clinically scored for four to six hours. Subsequently, mice were sacrificed, and blood and organs were collected for flow cytometric and histopathological analysis. To assess the impact of thrombocytopenia and neutrophil depletion on peritoneal hemorrhage, mice were injected with a platelet-depleting antibody (R300, emfret, 100 µg per mouse) intravenously, a neutrophil-depleting antibody (UltraLeaf anti-Ly6G, Biolegend, 100 µg per mouse) intraperitoneally 12 hours prior to NaCl or LPS administration. Depletion efficiency was analyzed by flow cytometry and automated cell counting. For assessment of inflammatory bleeding in the peritoneal cavity, mice were sacrificed and 8 ml of PBS containing 5% BSA and 0.25 mM EDTA were instilled using a 26G needle after careful incision of the abdominal skin. A 20G needle was used to collect as much peritoneal lavage fluid as possible. Inflammatory bleeding and leukocyte infiltration were subsequently assessed by flow cytometry and immunofluorescence staining.

Tail bleeding assay

Mice were anesthetized as described above. Hereafter, 5 mm of the distal tail was resected using a precision scissor (MST) and the tail was immediately placed in 40 ml PBS (room temperature). Bleeding and re-bleeding times were recorded for 20 min. Bleeding was further quantified by using an automated cell counter to assess hemoglobin content.

$FeCl_3$-induced arterial thrombosis (A. carotis)

Ferric chloride-induced arterial thrombosis was performed as previously described[4]. In brief, male mice were anaesthetized and a DyLight 488-conjugated Gp1b antibody (X488, emfret, 50 µl) was injected into the tail vein. Next, the right carotid artery was surgically exposed, and a small filter paper (0.5 mm^2) saturated with $FeCl_3$ solution (10%, Sigma Aldrich) was placed touching the proximal end of the exposed carotid proportion. The filter paper was removed after 3 min and the forming thrombus was visualized using a fluorescence microscope (AxioScope, Carl Zeiss), with images taken every 10 sec. After 30 min, the carotid containing the thrombus was retrieved for histological analysis.

GPVI depletion *in vivo*

For platelet-specific depletion and shedding of the collagen receptor GPVI, mice were injected with 100 µg of anti-GPVI antibody (clone JAQ1, emfret) i.p. Isotype-injected animals were used as controls. Subsequent experiments were initiated after 72 hours, when GPVI depletion remained sufficient and transient thrombocytopenia had resolved[5]. Efficacy of GPVI depletion was assessed by flow cytometric measurement of surface GPVI expression compared to isotype-treated animals as well as in platelet activation assays and flow cytometric measurement after stimulation with GPVI-specific agonist collagen and convulxin. Only animals with sufficient GPVI depletion were included in the respective experiments and analyses.

Platelet and neutrophil depletion *in vivo*

To deplete platelets, Bl6 mice were injected with 100 µg of an anti-Gp1b antibody (R300, emfret) i.v. immediately before or 12 hours prior to performing acute lung injury and peritoneal inflammation experiments, respectively. A non-immunogenic antibody mix (C301, emfret) was used as isotype control. For neutrophil depletion, 100 µg of an anti-Ly6G antibody (UltraLeaf anti-Ly6G, clone 1A8, Biolegend) were injected i.p. 12 hours prior to induction of LPS-mediated peritoneal inflammation; an isotype (UltraLeaf rat anti-mouse IgG2a, Biolegend, 100 µg) was used as control. Depletion efficiency of both platelets and neutrophils was assessed by flow cytometry.

Antibodies and fluorescence-coupled proteins for flow cytometry and histopathology

Antibodies and other fluorescent proteins or peptides are listed in Suppl. Table 1. Antibodies were used 1:100 for flow cytometric analysis unless otherwise stated. Secondary antibodies used for histopathology and immunofluorescence stainings were used 1:200. For previously unused antibodies in our lab, isotype control stainings were performed to ensure staining specificity. In addition to using fluorescence-coupled annexin V, Ca^{2+}-independent PS-staining reagent consisting of biotinylated C1 domains of murine lactadherin that have been multimerized using Strepatvidin. These C1 multimers (C1) were used for the detection of procoagulant platelets *in vitro* and *in vivo* and are commercially available through Biolegend (see above) and have been described by our group[6]. For the detection of caspase 3/7 activation in procoagulant platelets, the CellEvent kit (ThermoFisher, # C10423) was used (final concentration 20 µM). FITC: fluorescein isothiocyanate, PE: phycoerythrin, APC: allophycocyanin, AF: AlexaFluor, PB: pacific blue, BV: brilliant violet.

Multiplex cytokine measurements

Cytokine levels of murine plasma and BAL fluid sampled shown in Suppl. Figure 1D were assessed using the LEGENDplex™ Mouse Inflammation Panel (13-plex (Biolegend, #740446) according to the manufacturer's instructions. Samples were measured on a BD LSRFortessa flow cytometer and resulting MFIs were analyzed using the LEGENDplex™ Data Analysis Software Suite to assess approximate cytokine concentrations.

Human blood donors

Female and male volunteers aged 21 to 45 years served as donors for the isolation platelets, plasma samples or whole blood flow cytometry or thrombus formation experiments. All experiments involving human subjects are approved by a local ethical review board (LMU Munich), complying with any relevant regulation for experiments involving human samples.

Human and mouse platelet isolation

Human blood was drawn by venipuncture of the cubital into syringes containing acid-citrate dextrose (39 mM citric acid, 75 mM sodium citrate, 135 mM dextrose; ACD, 1/7 volumes) and immediately diluted 1:1 with modified Tyrode's buffer (137 mM NaCl, 2.8 mM KCl, 12 mM $NaHCO_3$, 5.5 mM sucrose, 10 mM HEPES, pH = 6.5). For mouse platelet isolation, all animals were anesthetized, and blood was subsequently collected by introduction of a glass capillary into the retroorbital vein plexus into 1/7 volumes of ACD followed by 1:1 dilution into Tyrode's buffer, pH 6.5. Both human and murine samples were subsequently centrifuged with 70g for 35 or 15 min, respectively, to generate platelet-rich plasma (PRP). To isolate platelets, PRP was diluted 1:2 in modified Tyrode's buffer supplemented with PGI_2 (0.1 mg/ml) and either albumin (0.1%) or casein (0.01%), and subsequently centrifuged for 5-10 min at 1000g. After

resuspending the pellet in Tyrode's buffer, platelet counts were assessed using a Sysmex XN-V Series XN-1000V cell counter. Platelet-poor plasma (PPP) was generated by centrifugation of PRP for 5 min at 14,000g.

Inhibitors and agonists

Cyclosporin A (#30024), niflumic acid (#N0630), Ru360 (#557440), Synta66 (SML1949), Thrombin (#T4648), E. coli-derived LPS O111:B4 (#L2630), adenosin diphosphate (ADP, #01905) and mP6 (#5098840001) were purchased from Sigma and MerckMillipore. The PAR4 inhibitor BMS-986120 was purchased from CaymanChem (#23497). All other inhibitors used and mentioned in Supplemental Data are described in detail by Nicolai et al.[4] The Syk inhibitor BI-1002494 and a control compound, BI-2492, were gifts from Boehringer Ingelheim. Clinical-grade tirofiban, enoxaparin and argatroban were purchased from ibigen, Sanofi-Aventis and Mitsubishi Pharma, respectively.

Chemicals

Horm collagen was purchased from Takeda (#1130630). Casein, human serum albumin, hexamethyldisilazane (HMDS), paraformaldehyde (PFA) and glutaraldehyde (GDA) were purchased from Sigma. Prostacycline (PGI_2) was ordered from abcam. Unconjugated and AF546- or AF488-conjugated fibrinogen as well as the calcium-binding compound Fluo-4 (#F14201) were acquired from ThermoFisher.

Migration and retraction assays

Isolated mouse and human platelets were diluted to a concentration of 150,000 – 200,000/µl. $4x10^6$ platelets were subsequently activated by the addition of 4 µM ADP, 2 µM U46619 and 1 mM calcium chloride, pipetted into pre-coated custom chambers and incubated for 15 min at 37°C. Hereafter, non-adherent cells were removed by three washing steps with cell-free wash buffer containing 1 mM calcium chloride and antibodies and/or compounds for detection of platelets and respective activation markers. After 30-60 min, cells were fixated with fixation mix containing 2% PFA and 0.005% GDA. Samples were imaged using either an epifluorescence (Olympus IX83 microscope) or a Zeiss LSM 880 confocal microscope. Per biological replicate, 5-6 random images were acquired. For live imaging of calcium oscillations, both murine and human isolated platelets were loaded with 1 µM Fluo-4 and allowed to seed for 15 min, washed three times and subsequently incubated for 10-15 minutes before imaging. Phase contrast, calcium oscillations and PS exposure were acquired every 10 seconds. In some instances, human PRP was loaded with 1 µM Fluo-4 for 20 min in the dark before centrifugation and isolation of washed platelets.

Live imaging of platelet migration, PS exposure and calcium signaling

Time-lapse video microscopy was performed using an inverted Olympus IX83 microscope with a 40x/1.0 or a 100x/1.4 oil-immersion objective and included recording of differential interference contrast (DIC), phase-contrast, and epifluorescence movies (5-20 s/frame). A pre-heated stage incubator (Tokai Hit) was used to mimic physiological conditions (humidified, 37°C). For live-imaging of calcium oscillations, human or murine PRP was loaded with 1 µM Fluo-4 (ThermoFisher) for 15 min at RT in the dark. Intensities of calcium oscillations and PS exposure were measured using Fiji ImageJ and quantified in a cell-based manner.

Thrombin turnover assay

Isolated mouse or human platelets were activated and left migrating on a collagen I/HSA/fibrinogen matrix as described above. After 15 min of migration, media were replaced by a solution containing PPP (20%) and a fluorescent thrombin substrate (13.3 µM final concentration, SensoLyte® 520 Thrombin Activity Assay Kit, Anaspec, #AS-72129) as well as an antibody against CD41 or CD42b and the C1 multimer to distinguish procoagulant from non-procoagulant platelets. Thrombin turnover was assessed by confocal imaging (Zeiss LSM 880). Thrombin positivity and procoagulant activation were assessed for at least 100 platelets from at least n = 2 individual mice and analyzed using Fiji ImageJ.

Pharmacological inhibition of platelet pathways and receptors

For testing of pathways involved in procoagulant activation of migrating and spreading platelets, inhibitors were added to the third and final washing step after platelets had adhered to the respective coating. Concentrations varied according to the compound used and are indicated in the respective figures and figure legends, with various concentrations being tested for all compounds (data not shown). In some cases (e. g. treatment with ciclosporine A), platelets were incubated with the respective compound or antibody for 15 min before being added to custom chambers. In case of dual receptor inhibition (e. g. GPIIBIIIA and GPVI), identical concentrations of individual compounds were used.

Platelet activation assay

Activation of platelets in suspension was performed as described previously[4]. In brief, isolated human or murine platelets suspended in modified Tyrode's buffer with 1 mM calcium chloride were incubated with fluorescent antibodies against platelet activation markers P-selectin, activated GPIIBIIIa and PS – among others – and activating agents targeting $P2Y_{12}$, thrombin receptors PAR2/4 (thrombin), GPVI (convulxin, collagen) and the thromboxane receptor TXA_2-R (U46119) for 30 min at RT or 37°C (concentrations indicated in the respective figures). Platelets were subsequently fixated with 1% PFA for 10 min in the dark, before being measured

on a BD LSRFortessa flow cytometer. Gating strategies are found in Suppl. Figure 9. Gating of subpopulations as well as MFI analyses were performed using FlowJo (v10).

Immunofluorescence staining

Platelets were fixated with fixation mix (PFA 2%, GDA 0.05%) for 10 min and subsequently stained using primary and secondary or primary-labelled antibodies in PBS containing 1% BSA for 1 h in the dark. In between primary and secondary antibodies as well as prior to imaging, platelets were washed three times with 1% BSA-containing PBS. Imaging was performed using a Zeiss LSM 880 confocal microscope in Airyscan mode (40/1.3 and 63/1.3 oil immersion objective).

Histopathological staining and analysis

For immunofluorescence and histopathological stainings, organs were first fixated in 4% PFA for 1 h at RT, dehydrated in 30% sucrose at 4°C overnight, cryoembedded and stored at either -80°C (long term storage) or -20°C (if processing was immediate). Organs were cut into 10 µm thick slices using a cryotome, fixated with 4% methylene-free PFA in PBS and subsequently permeabilized and blocked (10% goat serum, 0,5% saponin and 1% BSA in PBS). Samples were then stained using primary antibodies against TER119, Ly6G, CD42b, fibrinogen and phosphatidylserine as well as Hoechst dye to counterstain nuclei. Stained samples were imaged in Airyscan Super Resolution (SR) mode (20x/0.8 objective) on a Zeiss LSM 880 confocal microscope at 0.6x magnification. Random areas were acquired by focusing on nuclei without prior assessment of either bleeding or neutrophil infiltration to ensure objective measurement. Neutrophil and platelet recruitment were assessed using a custom-made macro in Fiji ImageJ, which uses a neutrophil- or platelet-specific size range to identify individual cells. Pulmonary hemorrhage as defined by extravascular TER119-positive areas was measured after thresholding and exclusion of intravascular erythrocytes from the image.

Data collection and visualization

Data from *in vivo* and *in vitro* live imaging experiments were collected using Fiji ImageJ[7]. For 4D *in vivo* timelapse microscopy, dimensions were reduced by maximum intensity projection. Assessment of motility patterns of platelets were defined as described by Nicolai *et al.*[4]. Migrating platelets from *in vitro* migration assays were tracked using the Fiji Manual tracking plugins, and were analyzed for directionality, velocity and acquired distance using the Chemotaxis Tool (ibidi) plugin. Shape analysis *in vitro* including platelet area, circularity and filopodia formation was performed described previously[4]. *In vivo*, motility patterns were defined as adherence, if platelets showed no distinguishable displacement over a duration of three acquired frames, leukocyte-dependent movement for platelets that showed movement while

in direct contact with CD45+ leukocytes and/or Ly6G+ neutrophils, respectively, and migration for movement of platelets along the vessel wall without contact to leukocytes and with displacement of at least one cell diameter during image acquisition. Procoagulant platelets were defined as CD42b-positive, balloon-like shapes that were platelet-like in size and stained positive for phosphatidylserine as assessed by Annexin V or mC1 multimer staining (see Figure 2B, C, Suppl. Figure 2A-E and Suppl. Video 1). Procoagulant platelets were counted as fibrinogen-positive if they exhibited an overlap between PS and fibrinogen channels (see Figure 2E, F, with yellow indicating channel overlap). In some cases, a line was manually drawn across a multi-channel image and MFIs of the respective fluorescence channels were analyzed and plotted using Fiji "plot profile" function. In *in vitro* migration assays that were imaged after fixation of cells, platelets were counted either in DIC/PH channels or a CD41 fluorescence channel. Platelets were defined as "migrating", if they had moved by at least one cell diameter as assessed by migration tracks in the fibrinogen channel. Procoagulant platelets were defined as having undergone morphological changes (ballooning, procoagulant spreading) and exposing PS as detected by Annexin V or C1 staining. In live imaging experiments, procoagulant platelets were considered positive for supramaximal calcium bursts if contact to collagen resulted in a calcium peak corresponding to at least 95% of the maximum fluorescence intensity. The cleared fibrinogen area, a surrogate for migration length, was analyzed by measuring the fibrinogen-negative area channel using Gaussian blur and thresholding in the fluorescent fibrinogen channel. Gaussian blurring, thresholding and area measurement were performed using a custom Fiji macro. For analysis of calcium oscillations of migrating platelets, measured Fluo-4 intensities and AnnV/C1 binding were normalized to 1) background fluorescence and 2) to % of maximum intensity to allow for comparison of live imaging videos collected at different days. In flow cytometry experiments, counting beads were used to normalize cell counts in both blood and BALF samples to counts per microliter of the respective sample. Individual graphs were generated using Prism v9 (Graphpad) and figures were generated using Illustrator 2021 (Adobe). Experimental schemes and the graphical abstract were designed using BioRender (www.biorender.com).

Statistical analysis

Data were analyzed using Prism v9 (Graphpad), Excel v16 (Microsoft) and FlowJo v10 (BD) and are visualized as mean ± standard deviation (SD); in selected graphs, data are depicted as SuperPlots[8], with single dots representing the single data points measured per replicate and error bars representing the SD of the mean from biological replicates. Unless otherwise stated, all data shown include at least three biological replicates, with at least 5-6 randomly taken, individual images underlying each biological replicate data point for imaging studies. Representative images or flow cytometry plots were chosen according to the mean value

represented in the respective data set. We estimated animal sample sizes according to power calculations performed when ethical approval of planned experiments was applied for. All experimental groups were matched according to age and sex of the respective mouse lines. Statistical differences between experimental groups were assessed using t-tests and analyses of variance (ANOVA) as stated in the respective figure legends. In experiments with uneven sample sizes across groups (e. g. due to death of animals in one experimental group), normality distribution of acquired data was ensured using Shaprio-Wilk tests prior to further statistical testing. Unless otherwise stated, experiments including more than two groups were tested using one-way ANOVA with post-hoc Holm-Šídák's multiple comparisons test compared to control groups. If different experimental conditions were assessed on the same biological replicate, paired t-tests were used; in all other cases unpaired t-testing was performed. All t-tests were two-sided. Across all statistical tests, a p-value of <0.05 was considered statistically significant; p-values were marked by asterisks as follows: * <0.05, ** <0.01, *** <0.005, **** <0.001, ns = non-significant. If no asterisks are indicated, there is no statistical difference between treatment groups.

Supplementary Tables

Suppl. Table 1: Antibodies and fluorescent proteins

Protein/epitope	Fluorophore	Target species	Manufacturer	Order #
act. CD42b (JonA)	PE	mouse	emfret	M023-2
Annexin V	FITC	-	Biolegend	640906
Annexin V	AF649	-	Biolegend	640912
Anti-mouse IgG	Cy3	mouse	Invitrogen	A10521
Anti-rabbit IgG	AF546	rabbit	Invitrogen	A11037
Anti-rabbit IgG	AF649	rabbit	Invitrogen	A21244
Anti-rat IgG	AF488	rat	Invitrogen	A21208
Anti-rat IgG	AF546	rat	Invitrogen	A11007
C301	-	mouse	emfret	C301
CD107a	BV785	mouse	Biolegend	328643
CD11b	BV605	human	Biolegend	101237
CD144	AF649	mouse	Biolegend	138006
CD15	APC	human	Biolegend	323008
CD31	AF649	mouse	Biolegend	102516
CD36	PE	mouse	Biolegend	102605
CD41	Pacific blue	human	Biolegend	303714
CD41	AF700	mouse	Biolegend	133926
CD42b	FITC	mouse	emfret	X488
CD42b	DyeLight-649	mouse	emfret	X649
CD42b	-	mouse	abcam	ab183345
CD44	AF700	mouse	Biolegend	103026
CD45	BV650	human	Biolegend	304044
CD45	PerCp-Cy5.5	mouse	Biolegend	103132
CD9	PE/Dazzle™ 594	mouse	Biolegend	124821
EpCAM	PE-Cy7	mouse	Biolegend	118216
Fibrinogen	-	-	BioRad	4440-8004
Fibrinogen	AF546	-	ThermoFisher	F13192
Fibrinogen	AF488	-	ThermoFisher	F13191
GPVI (JAQ1)	FITC	mouse	emfret	M011-0
Gr-1	AF488	mouse	Biolegend	108417
Hoechst Dye	-	-	ThermoFisher	H3570

Hoechst Dye	-	-	ThermoFisher	H3570
IgG2a (Ultra-LEAF™)	-	-	Biolegend	400565
Ly6G	PE	mouse	Biolegend	127608
Ly6G	PB	mouse	Biolegend	127612
Ly6G	BV711	mouse	Biolegend	127643
Ly6G (Ultra-LEAF™)	-	mouse	Biolegend	127649
mC1 multimer	Cy3	-	-	TBD
mC1 multimer	AF649	-	-	TBD
PAC-1	AF649	human	Biolegend	362806
P-selectin	BV421	human	Biolegend	304926
P-selectin	PE-Cy7	mouse	Biolegend	148310
P-selectin	PE	human	Biolegend	304905
Phosphatidylserine	-	-	Merck	05-719
R300	-	mouse	emfret	R300
Streptavidin	AF649	-	Biolegend	405237
Streptavidin	Cy3	-	Biolegend	405215
TER119	PE	mouse	Biolegend	116208
TER119	AF488	mouse	Biolegend	116215
Thrombin	5-FAM/QXL™ 520	-	Anaspec	AS-72129

Suppl. Table 2: Relative comparison of inflammatory bleeding severity

Mouse line/inhibitor	**Mean bleeding (% relative to LPS-treated control, ±SD)**
Platelet depletion (R300)	11093.89 ± 674.16
Argatroban (anti-FIIa)	160.76 ± 19.17
Rivaroxaban (anti-FXa)	146.69 ± 35.85
Enoxaparin (anti-FXa)	307.29 ± 70.21
PF4cre-CypD (Cre+)	287.30 ± 59.29
PF4cre-TMEM16F (Cre+)	473.21 ± 81.99
JAQ1 (anti-GPVI)	57.63 ± 22.19
Tirofiban (anti-GPIIBIIIA)	122.16 ± 42.24
JAQ1 + Tirofiban	162.39 ± 9.02
negative ctrl (NaCl i.n.)	5.90 ± 10.43

Supplementary Figure legends

Suppl. Figure 1: Anticoagulation aggravates inflammatory bleeding. | (A) Experimental scheme of subacute lung injury model, comparing intranasal LPS challenge (black arrow) with sham-treated animals. (B) Representative macroscopic image of BALF derived from experimental groups, collected in 2 ml Eppendorf tubes. (C) Flow-cytometric assessment of BALF RBC, neutrophil, platelet and platelet-neutrophil aggregate counts. n=4 animals per experimental group. Student's t-test, two-tailed, unpaired. (D) Quantification of cytokine measurements from plasma and BALF of sham- and LPS-treated animals collected 24 h hours after treatment. Two-way ANOVA with Holm-Šídák's multiple comparisons test. (E) Quantification of alveolar hemorrhage ($TER119^+$ area) and neutrophil recruitment in control (C301) and thrombocytopenic animals (R300) after LPS-induced lung injury, corresponding to Figure 1A-D. Student's t-test, two-tailed, unpaired. (F) Experimental scheme of subacute lung injury model with or without enoxaparin (ENOX)-mediated anticoagulation (s.c. injections of 10 mg/kg BW enoxaparin 0 and 6 hours (red arrows) after LPS challenge (black arrow)). (G) Representative macroscopic image of BAL fluid derived from experimental groups, collected in 2 ml Eppendorf tubes. (H) Flow-cytometric assessment of BALF RBC and leukocyte counts. Student's t-test, two-tailed, unpaired. (I) Clinical scores of individual animals for 24 h after LPS challenge treated with Rivaroxaban, Argatroban or vehicle. Sepsis scores contain appearance, activity, responsiveness and breathing patterns. One-way ANOVA with post-hoc Holm-Šídák's multiple comparisons test. (J) Flow-cytometric assessment of peripheral blood platelet and leukocyte counts as well as procoagulant platelets and platelet-neutrophil aggregates (PNA) post-treatment. One-way ANOVA with post-hoc Holm-Šídák's multiple comparisons test. (K) Quantification of platelet recruitment and platelet-neutrophil aggregate (PNA) formation per mm^2 lung, referring to Figure 1J-O. (L) Representative micrographs from immunofluorescence stainings of lung slices from mice treated with vehicle or 10 mg/kg BW enoxaparin. Scale bar 25 µm. (M) Quantification of alveolar hemorrhage ($TER119^+$ area), neutrophil and platelet recruitment. Student's t-test, two-tailed, unpaired. (N) Representative micrographs of migrating human platelets treated with vehicle, rivaroxaban (10 µg/ml) or argatroban (10 µg/ml). Scale bar 10 µm. (O) Quantification of % migrating platelets and the absolute cleared area per cell in $µm^2$ from n = 3 healthy individuals. One-way ANOVA with post-hoc Holm-Šídák's multiple comparisons test.

Suppl. Figure 2: The C1 multimer detects procoagulant platelets *in vitro* and *in vivo*. | (A) Representative micrograph of migrating human platelets stained with antibodies/compounds against CD42b (white) and phosphatidylserine (C1, red, and Annexin V, green). Scale bar 10 µm. (B) Quantification of PS staining positivity by C1 and Annexin V, n = 3 individual donors. Student's t-test, paired, two-tailed. (C) Quantification of % procoagulant

platelets (detected by C1 multimer) and AnnV MFI of human platelets after stimulation with indicated agonists. One-way ANOVA with with post-hoc Holm-Šídák's multiple comparisons test, compared to Ctrl. (D) Correlation of C1 MFI with AnnV MFI and CD41 MFI of human platelets from the same experiment. P-value of linear regression analyses indicates significantly non-zero. (E) Representative scatter plots of human platelets from the same experiment to identify procoagulant platelets in response to thrombin/convulxin dual stimulation with C1 (left panels) and AnnV (right panels), respectively. (F) Experimental scheme and micrographs of 4D live microscopy of an inflamed mesenteric venule, corresponding to Suppl. Video 1. Dashed lines indicate the vessel wall. PS staining: mC1. Scale bar 5 µm. (G) Representative micrograph and quantification of procoagulant platelet recruitment and overlap of fibrinogen/PS/platelet positive areas. n = 3-4 animals corresponding to Figure 1G, H. PS staining: anti-PS antibody (Merck). Student's t-test, two-tailed, unpaired. (H) Experimental scheme of peritoneal inflammation model with or without depletion of platelets and/or neutrophils through antibody injection (red arrow) 12 hours prior to NaCl or LPS injection i.p. (black arrow). (I) Representative image of peritoneal lavage fluid for indicated, LPS-treated experimental groups, contained in 15 ml collection tubes. (J) Flow cytometry-based quantification of peripheral platelet and neutrophil counts to confirm cell-specific depletion. One-way ANOVA with post-hoc Holm-Šídák's multiple comparisons test, compared to LPS-treated Isotype control group. (K) Flow cytometry-based quantification of peritoneal lavage RBC and leukocyte counts as well as % of neutrophils among peritoneal leukocytes. One-way ANOVA with post-hoc Holm-Šídák's multiple comparisons test, compared to LPS-treated Isotype control group. (L) Quantification of $TER119^{+}$ area in μm^2 and representative immunofluorescence images of mesenteric sections of thrombocytopenic mice i.p.-injected with NaCl (left panel) as well as LPS-challenged isotype- and R300-treated animals (center and right panels). White arrowheads indicate extravascular microbleeding. One-way ANOVA with post-hoc Holm-Šídák's multiple comparisons test, compared to LPS-treated Isotype control group. Scale bar 100 µm. (M) Quantification and representative immunofluorescence imaging of intravascular fibrin(ogen) deposition in mesenteric vessels of LPS-challenged animals treated with isotype or anti-Ly6G antibody. Student's t-test, two-tailed, unpaired. Scale bar 25 µm. (N) Representative micrograph of the mesenteric vasculature, corresponding to Figure 2J. Scale bar 20 µm.

Suppl. Figure 3: Supporting data migration assay (I). | (A) Representative images from migration assays of both Cre-positive and -negative murine platelets isolated from PF4cre-$Arpc2^{fl/fl}$ animals. White arrowheads indicate migrating platelets turning procoagulant. Scale bar 10. (B) Quantification of procoagulant activation from mouse platelets seeded on fibrinogen or collagen I mono-coatings. Student's t-test, unpaired, two-tailed. (C) Flow-cytometric

quantification of relative MFIs of P-selectin expression, GPIIBIIIA integrin activation and PS exposure (mC1) by both Cre-positive and -negative murine platelets isolated from PF4cre-Arpc2$^{fl/fl}$ animals after exposure to indicated agonists. Two-way ANOVA with post-hoc Holm-Šídák's multiple comparisons test, compared to PBS control group. (D) Representative scatter plots of flow cytometry experiments with isolated murine WT platelets incubated with PBS or collagen I; quantification of P-selectin-positive platelets and PS MFI (mC1) for platelets from n=4 mice. Student's t-test, unpaired, two-tailed. (E) Relative quantification of procoagulant platelet formation in the presence or absence of fibrinogen after stimulation with PBS, collagen I or convulxin and thrombin. Human platelets from n = 4 healthy donors. One-way ANOVA. (F) Relative quantification of fibrinogen-positive platelets and absolute quantification of mean fluorescence intensities (MFIs) of platelet-bound fibrinogen-AF488 after stimulation with PBS, collagen or convulxin and thrombin. Right panel: representative scatter plots. Human platelets from n = 4 healthy donors. One-way ANOVA with post-hoc Holm-Šídák's multiple comparisons test, compared to PBS control group. (G) Relative quantification of procoagulant platelet activation and cleared area from n=3 migration assays with human platelets incubated with PBS or a combination of Cangrelor (0.25 µM), Terutroban (1 µg/ml), and Vorapaxar (1 µM). Student's t-test, unpaired, two-tailed. (H) Quantification of procoagulant platelet activation and cleared area from n=4 migration assays with human platelets incubated with PBS, PAR1 inhibitor Vorapaxar (1 µM), PAR4 inibitor BMS-986120 (1 µM) or a combination of both inhibitors. One-way ANOVA with post-hoc Holm-Šídák's multiple comparisons test, compared to PBS control group. (I, J) Representative micrographs of migrating human platelets on a hybrid matrix. Red (anti-Fbg antibody, anti-Sheep secondary antibody coupled to AF649) indicates all fibrin(ogen), including endogenous (platelet-inherent) and exogenous (Fbg-AF488, used for coating) fibrin(ogen); yellow indicates overlap of both channels. The arrowhead indicates overlap of both stainings, the white star indicates red-only and thus endogenous fibrin(ogen) deposition next to a procoagulant platelet. PS-detecting agent: C1-Cy3. Scale bars 20 µm (I), 2 µm (J).

Suppl. Figure 4: Validation of PF4cre-CypD$^{fl/fl}$ and PF4cre-TMEM16F$^{fl/fl}$ mouse lines. | (A) Baseline quantification of body weight and peripheral platelet, RBC and leukocyte counts of PF4cre-CypD$^{fl/fl}$ mice, n=4 per Cre-positive/-negative animals. Student's t-test, unpaired, two-tailed. (B) Flow-cytometric analysis of baseline expression of several platelet receptors from isolated platelets. n=4 per Cre-positive/-negative animals of the PF4cre-CypD$^{fl/fl}$ mouse line. Two-way ANOVA. (C) Flow-cytometric quantification of absolute MFIs of P-selectin expression, GPIIBIIIA integrin activation and PS exposure (stained by C1) by both Cre-positive and -negative murine platelets isolated from PF4cre-CypD$^{fl/fl}$ animals after exposure to indicated agonists. n=4. Two-way ANOVA. (D) Baseline quantification of body weight and

peripheral platelet, RBC and leukocyte counts of PF4cre-TMEM16F$^{fl/fl}$ mice, n=3-4 per Cre-positive/-negative animals. Student's t-test, unpaired, two-tailed. (E) Flow-cytometric analysis of baseline expression of several platelet receptors from isolated platelets. n=4 per Cre-positive/-negative animals from PF4cre-TMEM16F$^{fl/fl}$ mice. Two-way ANOVA. (F) Flow-cytometric quantification of absolute MFIs of P-selectin expression and PS exposure (stained by C1) by both Cre-positive and -negative murine platelets isolated from PF4cre-TMEM16F$^{fl/fl}$ animals after exposure to indicated agonists. n=3-4. Two-way ANOVA. (G) Quantification of total bleeding time and time to first hemostasis of Cre-positive and -negative PF4cre-CypD$^{fl/fl}$ mice. n = 5-7 per group. Student's t-test, unpaired, two-tailed. (H) Quantification of total bleeding time and time to first hemostasis of Cre-positive and -negative PF4cre-TMEM16F$^{fl/fl}$ mice. n = 4-8 per group. Student's t-test, unpaired, two-tailed. (I) Analysis of arterial thrombosis experiments with PF4cre-CypD$^{fl/fl}$ mice (n = 7 for both Cre- and Cre+ mice) with quantification of time to first occlusion, % of vessel occlusion, maximum thrombus size as well as longitudinal assessment of % of occlusion-free vessels over time. (J) Representative images of carotid arteries from Cre+ and Cre- PF4cre-CypD$^{fl/fl}$ mice after 3 min of $FeCl_3$-induced injury at maximum thrombus size. Dashed lines represent vessel walls. Scale bar = 500 µm. (K) Analysis of arterial thrombosis experiments with PF4cre-TMEM16F$^{fl/fl}$ mice (n = 4-5 for both Cre- and Cre+ mice) with quantification of time to first occlusion, % of vessel occlusion, maximum thrombus size as well as longitudinal assessment of % of occlusion-free vessels over time. (L) Representative images of carotid arteries from Cre+ and Cre- PF4cre-TMEM16F$^{fl/fl}$ mice after 3 min of $FeCl_3$-induced injury at maximum thrombus size. Dashed lines represent vessel walls. Scale bar = 500 µm. (M) Representative micrographs of procoagulant activation of Cre-negative (left panels) and Cre-positive murine platelets (right panels) of PF4cre-TMEM16F$^{fl/fl}$ animals. PS staining: mC1. Scale bars 5 µm. (N) Cell-based quantification of the number of filopodia, number of released microvesicles and MFI of PS exposure of Cre-positive and -negative platelets isolated from PF4cre-TMEM16F$^{fl/fl}$ animals. Student's t-test, unpaired, two-tailed. (O) Representative micrograph of migrating and procoagulant mouse platelets that were co-stained for caspase activation using CellEvent™ Caspase-3/7 detection dye, showing caspase activation (red) in some procoagulant platelets. White arrowhead indicates a procoagulant, caspase-positive platelets, stars indicate migrating, caspase-negative platelets. Note that most procoagulant platelets are caspase-negative. Scale bar 20 µm. (P) Quantification of migrating and procoagulant mouse platelets for co-staining of PS (C1) and caspase activation. FOV-based quantification including 435 cells. One-way ANOVA with post-hoc Holm-Šídák's multiple comparisons test. (Q) Quantification of procoagulant activation and migratory capacity of platelets isolated from n = 3 WT mice with or without treatment with the pan-caspase inhibitor Q-VD-OPh (QVD, 50 µM). Student's t-test, unpaired, two-tailed. (R) Representative micrographs of migrating or procoagulant platelets:

migrating platelet from PF4cre mouse (Cre-positive, left panel), procoagulant platelet from PF4cre mouse (Cre-positive, center panel) and procoagulant platelet from PF4cre-TMEM16F$^{fl/fl}$ mouse (Cre-positive, left panel). PS staining: mC1. Scale bars 5 µm.

Suppl. Figure 5: Supporting data CypD/TMEM16F ALI experiments. | (A) BAL fluid neutrophil and platelet-neutrophil aggregate counts of PF4cre-CypD$^{fl/fl}$ animals 24 h after LPS challenge. Student's t-test, unpaired, two-tailed. (B) Peripheral platelet and leukocyte counts of PF4cre-CypD$^{fl/fl}$ animals 24 h after LPS challenge. Student's t-test, unpaired, two-tailed. (C) BAL fluid neutrophil and platelet-neutrophil aggregate counts of PF4cre-TMEM16F$^{fl/fl}$ animals 24 h after LPS challenge. Student's t-test, unpaired, two-tailed. (D) Peripheral platelet and leukocyte counts of PF4cre-TMEM16F$^{fl/fl}$ animals 24 h after LPS challenge. n = 4 animals per group. Student's t-test, unpaired, two-tailed.

Suppl. Figure 6: Supporting data mechanosensing and calcium imaging. | (A) Representative micrographs of isolated human platelets migrating on a fibrinogen/albumin matrix. Right panel: Representative calcium oscillations of migrating platelets. (B) Relative quantification of percentage of platelet procoagulant activation of all collagen-associated cells. Individual dots represent percentages derived from individual time-lapse microscopy videos. Platelets were isolated from n=2-3 mice per group. One-way ANOVA with post-hoc Holm-Šídák's multiple comparisons test. (C) Representative calcium (Fluo-4, green) and PS (mC1, pink) intensity profiles derived from live imaging of platelets from TMEM16F-deficient platelets. Arrows indicate the beginning of procoagulant activation after sensing collagen fibers, numbers indicate the time to supramaximal calcium plateau in seconds. (D) Quantification of time to calcium plateau for procoagulant platelets isolated from mice with indicated genotypes. n = 25 individual procoagulant platelets. One-way ANOVA with post-hoc Holm-Šídák's multiple comparisons test. (E) Representative micrographs of isolated platelets from CypD-deficient mice migrating on a fibrinogen/albumin/collagen I matrix, corresponding to Figure 6E. Scale bar 10 µm. (F) Quantification of procoagulant platelet activation and cleared area (as a proxy of migratory capacity) of human platelets treated with Synta66 (50 µM), Ru360 (50 µM) and BI-74932 (50 µM) to inhibit store-operated calcium entry (SOCE), mitochondrial calcium uniport and extracellular calcium influx, respectively. n = 3 healthy human donors. (G) Relative quantification of procoagulant platelet activation and cleared area per cell for human platelets (n=7) incubated with all the above calcium inhibitors (Synta66, Ru360 and BI-74932), normalized to untreated control platelets. Student's t-test, unpaired, two-tailed.

Suppl. Figure 7: Supporting data migration assay (II). | (A, B) Representative micrographs and quantification of migrating human platelets (n=3) on a hybrid collagen matrix with co-

staining of activated GPIIBIIIA by PAC-1 antibody. Arrowhead indicates migrating platelet with PAC-1 binding to the fibrin(ogen)-rich platelet's pseudonucleus. Note that only few procoagulant platelets bind PAC-1. Scale bar 20 µm. Student's t-test, unpaired, two-tailed. (C, D) Relative quantification of procoagulant platelets and cleared area from migration assays performed with human platelets from n = 3 healthy donors. Final concentrations for Ca^{2+} were 1 mM, unless calcium was depleted or not added to the assay. Inhibitor concentrations: PP2 20 µM, NSC27633 5 µM, U73122 10 µM, ML7 50 µM, Blebbistatin 1 µM. One-way ANOVA with post-hoc Holm-Šídák's multiple comparisons test compared to Ctrl group. (E) Representative micrographs of human platelets treated with the respective agonists/inhibitors, with the yellow outline indicative of the manual tracking of cell shape. Scale bar 3 µm. (F) Analysis of area, circularity and number of filopodia per platelet for n > 30 platelets per condition. One-way ANOVA with post-hoc Holm-Šídák's multiple comparisons test compared to control group. (G) Quantification of % migrating platelets and cleared area/platelet by murine platelets treated or not with 20 µM mP6. Student's t-test, unpaired, two-tailed. (H) Quantification of migrating platelets and cleared area/platelet by murine platelets treated or not with ascending concentrations of anti-GPVI antibody JAQ1. One-way ANOVA with post-hoc Holm-Šídák's multiple comparisons test compared to control group. (I) Quantification of migrating platelets and cleared area/platelet by murine platelets treated or not with ascending concentrations of Syk inhibitor BI-1002494. One-way ANOVA with post-hoc Holm-Šídák's multiple comparisons test compared to control group. (J) Quantification of migrating platelets, procoagulant activation and cleared area from migration assays with platelets from n = 3 human donors treated or not with the alpha2beta1 receptor inhibitor TC-I15 (10 µM). (K) Fluorescence microscopy image of migrating platelets, t = 16 min, corresponding to Figure 7D und Suppl. Video 3. PS staining: mC1. Scale bar = 10 µm. (L) Relative quantification of calcium amplitude of migrating platelets treated with vehicle, mP6 (20 µM) or BI-1002494 (2.5 µM). n=5-6 videos from n=2-3 mice per condition with a total of > 100 platelets were analyzed.

Suppl. Figure 8: Supporting *in vivo* and *in vitro* data for GPIIBIIIA and GPVI blockade. | (A) Representative confocal images of mouse platelets treated with isotype control and vehicle or JAQ1 (10 µg/ml) and tirofiban (1 µg/ml). PS staining: mC1. Scale bar = 10 µm. (B) Quantification of procoagulant platelet activation, migrating platelets and cleared area per platelet for indicated treatments. One-way ANOVA. (C) Representative scatter plots from flow cytometric measurements of isolated platelets from mice treated with the GPVI-blocking antibody JAQ1 or IgG2a isotype control (100 mg per animal injected i.p. 72 hours prior to platelet isolation). (D) MFIs for GPVI measured in platelets isolated from JAQ1- or IgG2a-treated Bl6 mice. Student's t-test, unpaired, two-tailed. (E) MFIs for PS (C1), P-selectin and activated GPIIBIIIA (JonA) after pre-incubation of human platelets with PBS or the GPIIBIIIA

antagonist tirofiban (1 µg/ml) and subsequent treatment with PBS or convulxin. One-way ANOVA. (F) Representative scatter plots from flow cytometric measurements of isolated human platelets after pre-treatment mit PBS or tirofiban and subsequent activation with convulxin. (G) Analysis of migrating platelets, procoagulant activation and cleared area of human platelets from n = 4 healthy human donors with or without tirofiban treatment (1 µg/ml). (H) Clinical scores of individual animals across treatment groups for 24 h after LPS challenge. Sepsis scores contain appearance, activity, responsiveness and breathing patterns. One-way ANOVA. (I) MFIs of several platelet receptors measured in whole blood of animals from treatment groups 24 h after LPS challenge. (J) MFI of GPVI in whole blood of mice from treatment groups 24 h after LPS challenge. One-way ANOVA. (K) Quantification of PNA formation in BAL fluid across treatment groups. One-way ANOVA. (L) Experimental scheme for peritoneal sepsis in Bl6 mice treated with JAQ1, a GPVI-blocking antibody, or isotype (red arrow) 72 hours prior to LPS challenge (black arrow) and vehicle or Tirofiban injections at 0 and 3 hours (red arrows) after LPS challenge. (M) Quantification of platelet GPVI expression, % procoagulant platelets and CD41 expression in whole blood across experimental groups (n=4). Student's t-test, two-tailed, unpaired. (N) Quantification of RBC and WBC counts as well as PNA formation in peritoneal lavage fluid (n=4). Student's t-test, two-tailed, unpaired. (O) Representative immunofluorescence stainings from mesenteric sections of control and JAQ1/tirofiban-treated animals, showing procoagulant (white arrowhead) and PS-negative platelets (white star) adherent to CD31-positive endothelium. Scale bar = 10 µm. (P) Quantification of platelet recruitment (number of all adherent vascular platelets) and % procoagulant platelets in mesenteric vessels of isotype/vehicle or JAQ1/tirofiban-treated animals after LPS administration (n=4). Student's t-test, two-tailed, unpaired. (Q) Representative immunofluorescence stainings from mesenteric sections of control and JAQ1/tirofiban-treated animals, revealing mesenteric microbleeding in dual blockade of GPVI and GPIIBIIIA (white arrowhead). Scale bar 50 µm. (R) Quantification of mesenteric microbleeding as assessed by extravascular RBC count per mm^2 mesentery. Student's t-test, two-tailed, unpaired. Holm-Šídák's multiple comparisons tests compared to control group were used for all one-way ANOVAs in this figure.

Suppl. Figure 9: Gating strategies for whole blood and BAL fluid. | (A) Representative scatter plots from whole blood with gating strategies for the identification of platelets, procoagulant platelets, leukocytes, neutrophils and neutrophil-platelet aggregates. MFIs were measured after gating for the respective population. (B, C) Representative scatter plots from BAL fluid with gating strategies for the identification of leukocytes, neutrophils and red blood cells. Peritoneal lavage samples (not shown) were gated according to the strategy shown in C.

Supplementary Video legends

Suppl. Video 1: Platelet procoagulant activation *in vivo*. 4D live microscopy of a mesentery venule. White: platelets, fire: PS exposure (mC1). Dotted lines indicate the vessel wall. Scale bar 10 µm.

Suppl. Video 2: Supramaximal calcium bursts prior to platelet ballooning and PS exposure of migrating platelets. Live microscopy of migrating human platelets on a hybrid albumin/fibrinogen/collagen I matrix. Phase contrast. Green: Fluo-4 (intracellular calcium oscillations), fire: PS exposure (AnnV). Scale bar 10 µm.

Suppl. Video 3: Calcium oscillations in migrating platelet pre-treated with mP6. Live microscopy of migrating human platelets on a hybrid albumin/fibrinogen/collagen I matrix. Phase contrast. Green: Fluo-4 (intracellular calcium oscillations), fire: PS exposure (mC1). Scale bar 10 µm.

Suppl. References

1. Tiedt R, Schomber T, Hao-Shen H, Skoda RC. Pf4-Cre transgenic mice allow the generation of lineage-restricted gene knockouts for studying megakaryocyte and platelet function in vivo. *Blood*. 2007;109(4):1503-1506.
2. Suzuki J, Fujii T, Imao T, Ishihara K, Kuba H, Nagata S. Calcium-dependent phospholipid scramblase activity of TMEM16 protein family members. *J Biol Chem*. 2013;288(19):13305-13316.
3. Fujii T, Sakata A, Nishimura S, Eto K, Nagata S. TMEM16F is required for phosphatidylserine exposure and microparticle release in activated mouse platelets. *Proc Natl Acad Sci U S A*. 2015;112(41):12800-12805.
4. Nicolai L, Schiefelbein K, Lipsky S, et al. Vascular surveillance by haptotactic blood platelets in inflammation and infection. *Nat Commun*. 2020;11(1):5778.
5. Schulte V, Rabie T, Prostredna M, Aktas B, Gruner S, Nieswandt B. Targeting of the collagen-binding site on glycoprotein VI is not essential for in vivo depletion of the receptor. *Blood*. 2003;101(10):3948-3952.
6. Rausch L, Lutz K, Schifferer M, et al. Binding of phosphatidylserine-positive microparticles by PBMCs classifies disease severity in COVID-19 patients. *J Extracell Vesicles*. 2021;10(14):e12173.
7. Schindelin J, Arganda-Carreras I, Frise E, et al. Fiji: an open-source platform for biological-image analysis. *Nat Methods*. 2012;9(7):676-682.
8. Lord SJ, Velle KB, Mullins RD, Fritz-Laylin LK. SuperPlots: Communicating reproducibility and variability in cell biology. *J Cell Biol*. 2020;219(6).

Suppl. Figure 1: Anticoagulation aggravates inflammatory bleeding

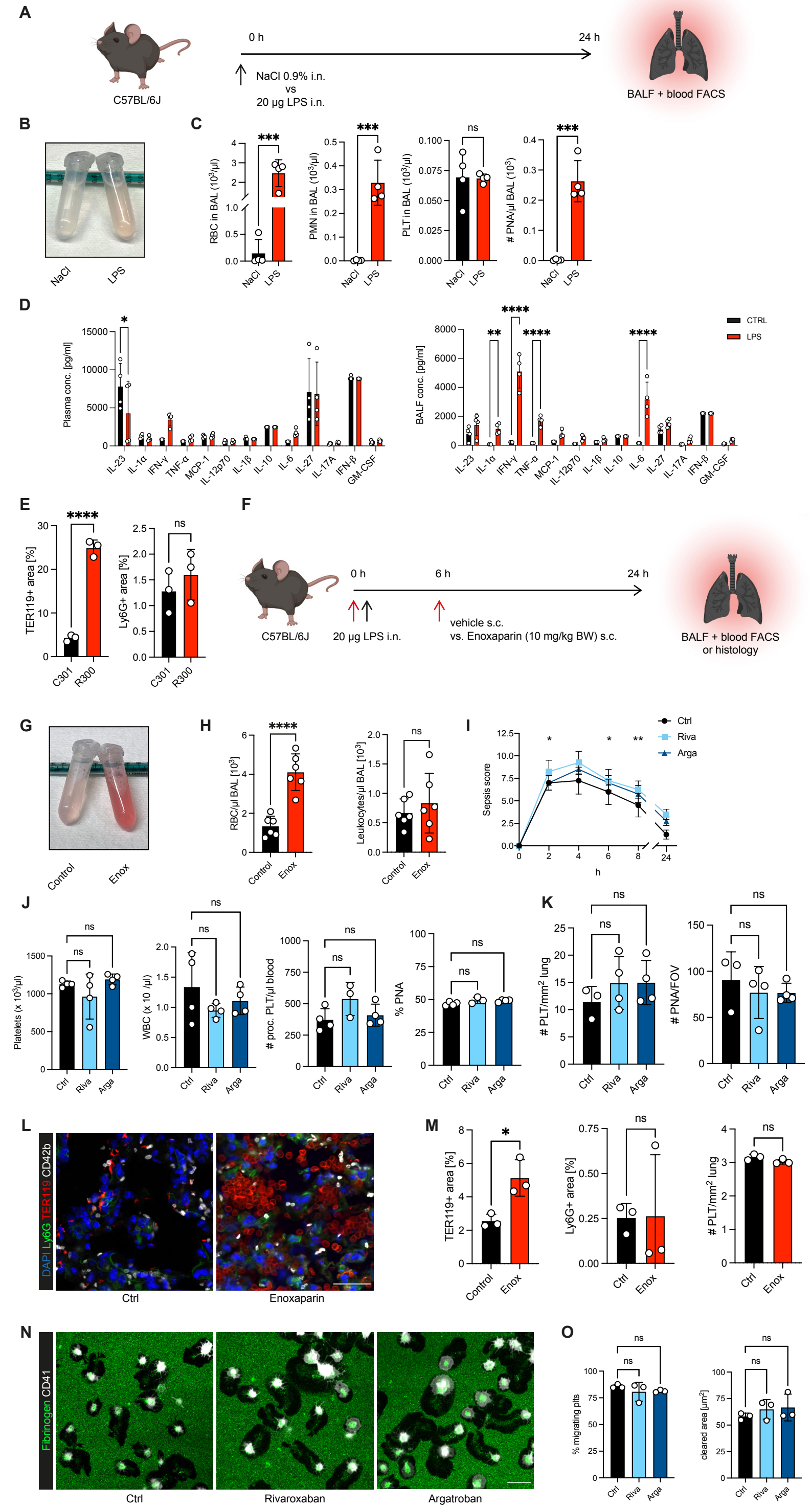

Suppl. Figure 2: The C1 multimer detects procoagulant platelets *in vitro* and *in vivo*

Suppl. Figure 3: Supporting data migration assay (I)

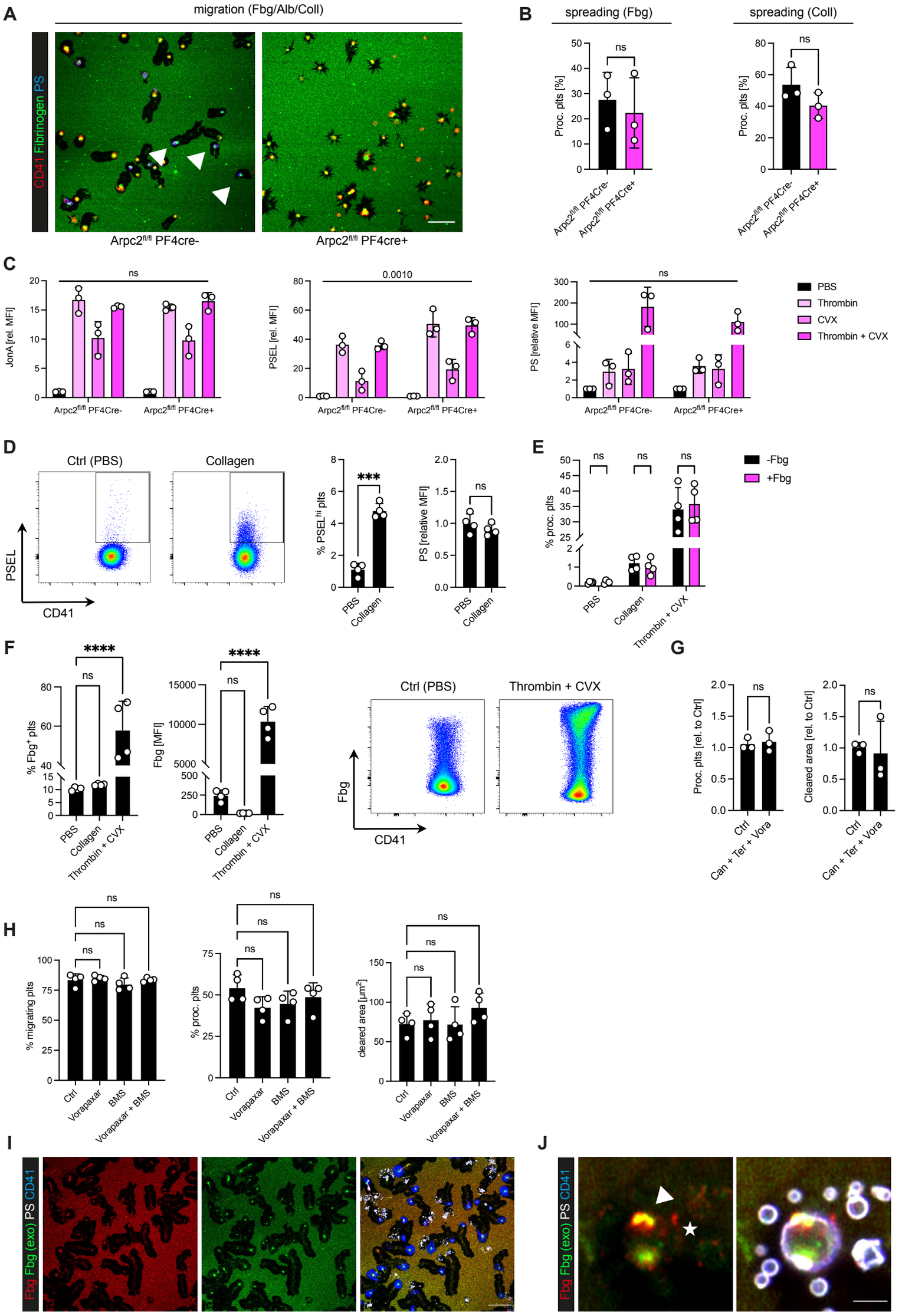

Suppl. Figure 4: Validation of PF4cre-CypD$^{fl/fl}$ and PF4cre-TMEM16F$^{fl/fl}$ mouse lines

Suppl. Figure 5: Supporting data CypD/TMEM16F ALI experiment

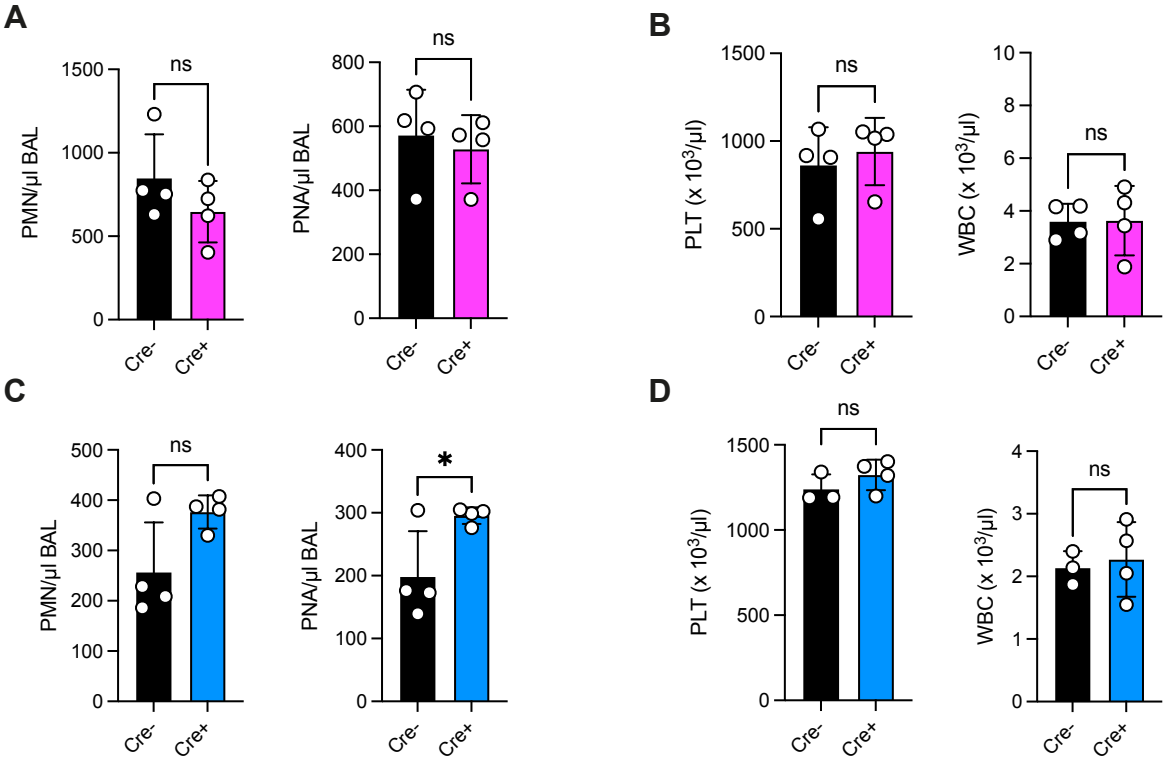

Suppl. Figure 6: Supporting data mechanosensing and calcium signaling

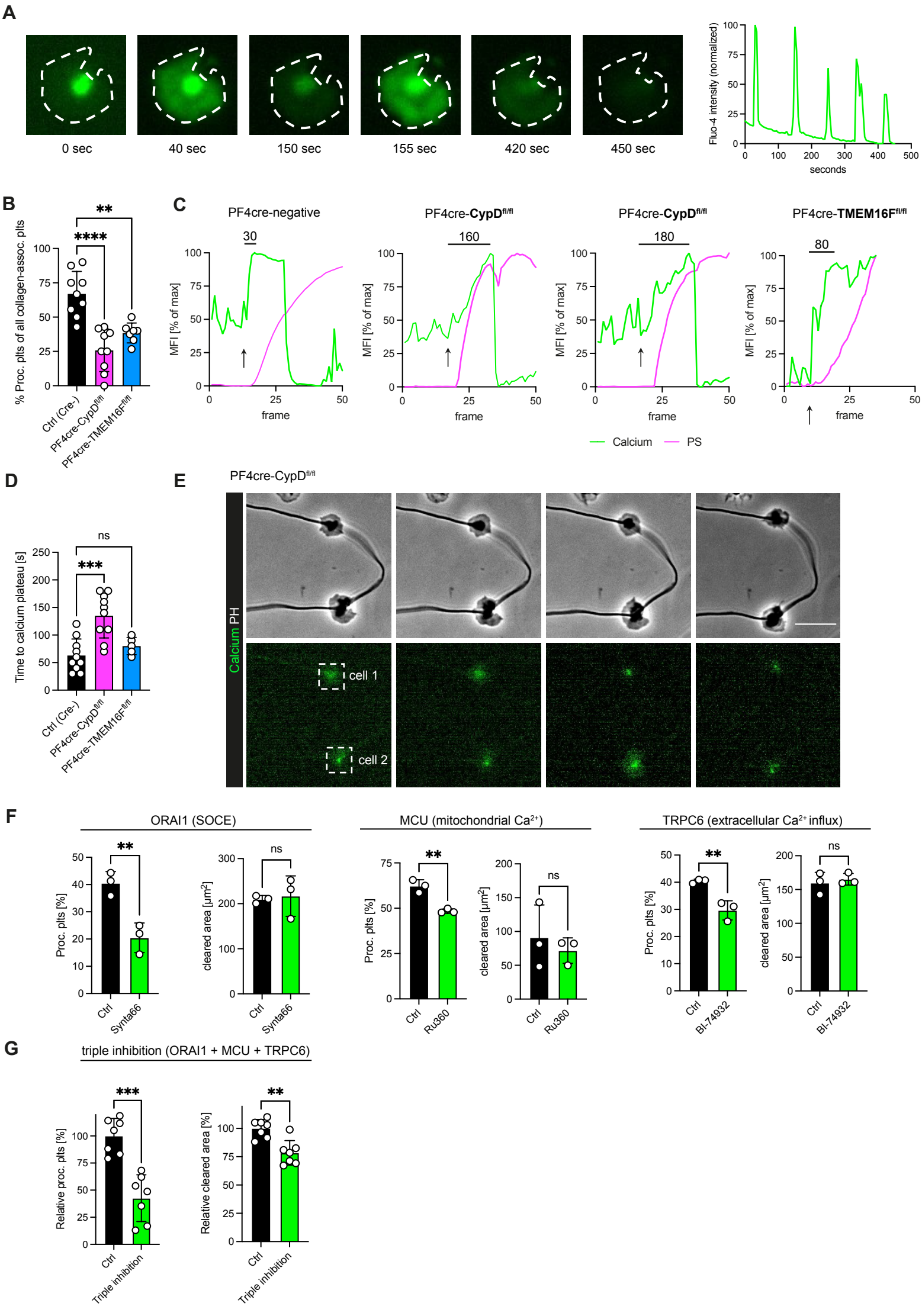

Suppl. Figure 7: Supporting data migration assay (II)

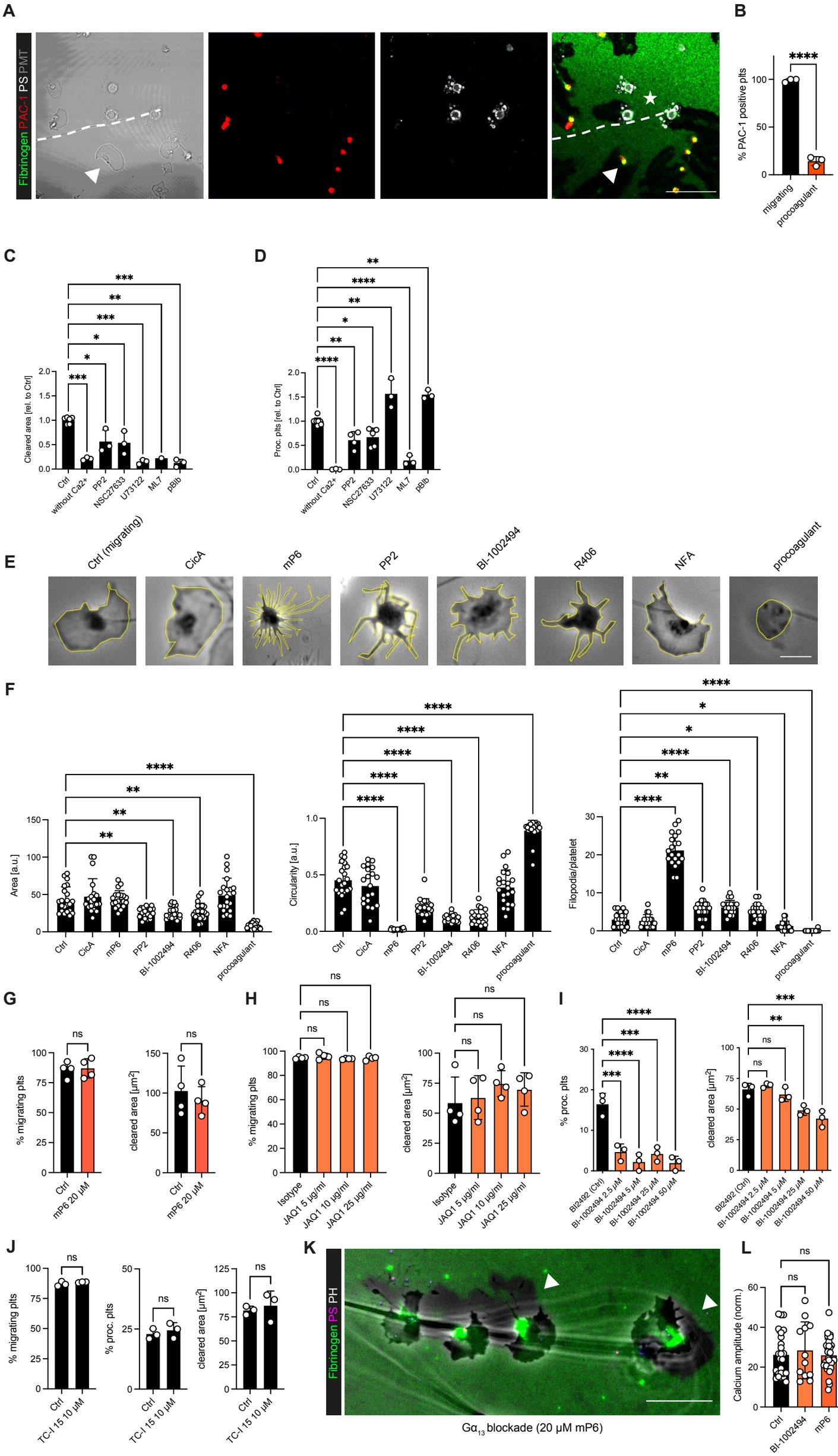

Suppl. Figure 8: Supporting *in vivo* and *in vitro* data for GPIIBIIIA and GPVI blockade

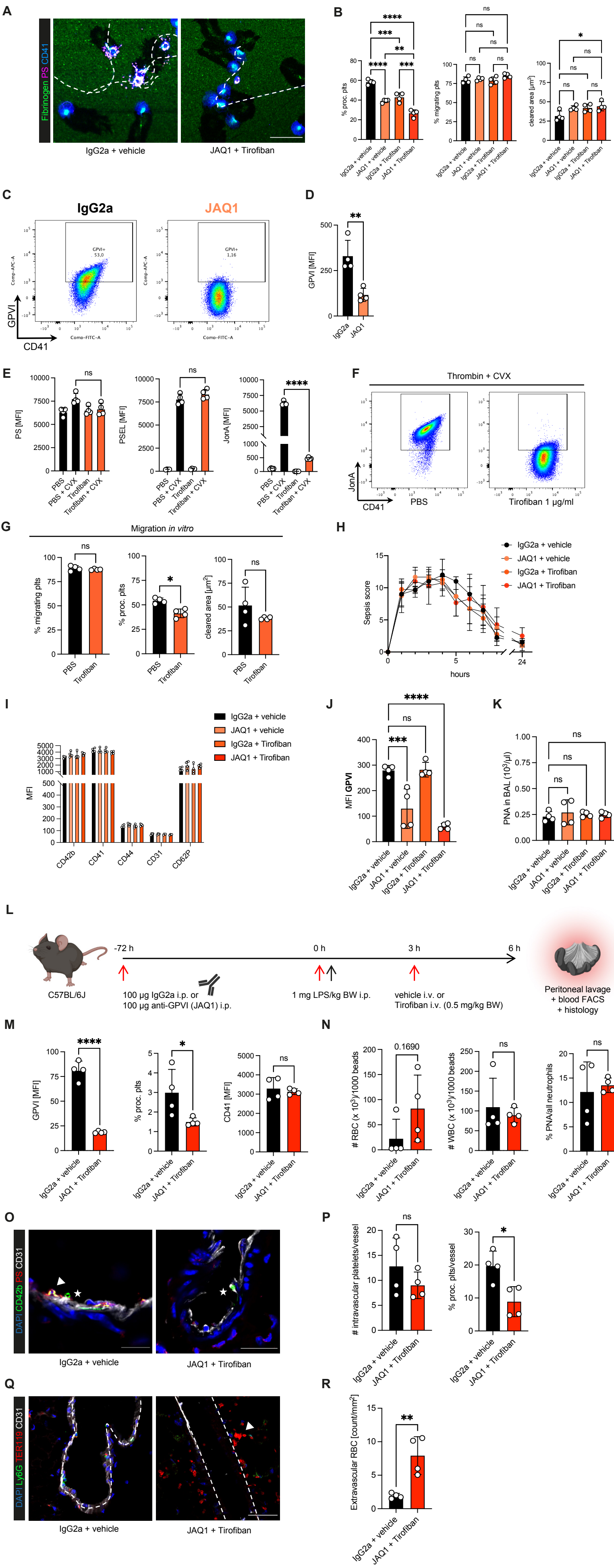

Suppl. Figure 9: Gating strategies